Composites and Nano Engineering (2022)
Clausius Scientific Press, Canada

DOI: 10.23977/compne.2022.010101
ISSN 2523-9015 Vol. 1 Num. 1

Postsynthetic Modification of Metal Organic Frameworks with Substituted Layered Double Hydroxides for Adsorption of Lead Ions

C.Y. Abasi[1, a, *], E. B. AttahDaniel[2, 3, b], F.M. Mtunzi[3, c], E.D. Dikio[1, d]

1. Department of Chemical Sciences, Niger Delta University, Bayelsa State, Nigeria.

2. Department of Chemical Sciences, Federal University Wukari, Taraba State, Nigeria.

3. Department of Chemistry, Faculty of Applied and Computer Sciences, Vaal University of Technology, P. O. Box X021, Vanderbijlpark, South Africa.

a. abasicy@yahoo.com, b. emmanuelabe@gmail.com c. fayana@vut.ac.za

d. ezekiel.dikio@gmail.com

**Corresponding author*

Keywords: Postsynthetic, modification, adsorption, ex situ, characterisation**,** layered double hydroxide, metal organic framework, isotherms,

Abstract: The effect of a two-pot postsynthetic modification of MOF with a modified LDH on the adsorption of Pb ions was investigated. Co-MOF was postsynthetically modified with an amino- silane substituted LDH and applied for the adsorption of Pb from aqueous solution. Synthetic and postsynthetic products were characterized by FTIR, PXRD and TGA/DTA. Blueshifts and redshifts of existing FT-IR bands in the PSM product in relation to that of the precursors confirmed the modification. PSM product was stable at temperatures up to 400ºC after a slight loss of surface water at low temperatures Adsorption capacity with respect to time at equilibrium was 34.58 mg/g, representing 87% of adsorbate uptake by the PSM Co-MOF. Equilibrium sorption data was better correlated by the Temkin model with a heat of sorption at 33.72 J/mol. Kinetic modelling was most favoured by the pseudo second order, and diffusion by film diffusion model.

1. Introduction

As the scale of industrialisation and technology soars to meet up social and economic demands, the side effects of effluent wastes remain a thing of concern to stakeholders and the public[1, 2]. While chemical substances used for industrial production and processes provide significant and helpful human application, their environmental effects leave less to be desired[3, 4]. For this reason, much attention has been and is still given to the synthesis or preparation of new materials to confront the challenge of environmental chemical pollutants such as heavy metals and soluble organic effluents[5].

Metal-organic frameworks [6] are a class of compounds that has received great attention for various applications such as gas adsorption, catalysis, separation, drug delivery[7]. The crystalline and porous structure of the MOFs make them suitable compounds for such applications[8]. Their open structure makes them accessible to other reactants resulting in modulated derivatives that can have improved properties[9]. In addition to the different synthetic approaches, chemical modification of already prepared MOFs has also gained attention over the years[7]. Structures of MOFs prepared by in-situ or ex-situ designs could be enhanced for better application by composing with organic function or metal ions.

Layered double hydroxides[6] are natural or synthetic anionic clays with sheets of hydroxides of divalent or trivalent metal ions whose charges are counterbalanced by anions found together with water molecules in the interlayer. They have the general formula $[M^{2+}_{1-x}M^{3+}_{x}(OH)_2]^{x+}[A^{n-}]_{x/n}.nH_2O$, where M^{2+} and M^{3+} are divalent and trivalent metal cations respectively; A^{n-} is an interlayer anion of charge n and x is the molar fraction of the trivalent cation, $M^{3+}/[M^{2+} + M^{3+}]$ with the value range of $0.2 < x < 0.33$[10]. Their two dimensional, layered crystalline structure provides sites and surfaces for insertion of guest molecules and ions through functionalisation, modification and ion exchange methods. Thus their structural modification with other moieties can result in useful composites for various applications[11] [12].

MOFs and LDHs have in the recent past been combined to form nanocomposites for various applications[6] [13]. The most widely used method for preparing these nanocomposites is the in situ precursor conversion method [14] [15], in which the precursors of the MOF are mixed with the as-prepared LDH under set conditions to form the composite of the LDH/MOF. However, ex situ methods involving the direct chemical linkage of the as-prepared products are rare. The postsynthethic modification[16] is an ex situ method that brings together prepared compounds with the intent of overcoming the effects of functionalities in porous materials [17]. While there are some works on the hybridization [8] [13], few literature exist in the area of composites of MOFs and LDHs obtained by postsynthetic modification. Procedures involving in-situ precursor conversion obtained the postsynthetic modified composite of ZIF-8-ZnAl-NO_3 [18].

In this paper, we describe the ex situ postsynthetic modification of Co–metal-organic framework (Co-MOF) by an amine-silane modified CoZnAl Layered double hydroxide (LDH) for a composite applied for the removal of Pb from aqueous solution.

2. Materials and Methods

2.1 Materials

Analytical grade reagents were used throughout this study. Cobalt nitrate hexahydrate (Riedel-deHaen, Germany), Zinc nitrate hexahydrate Merck, Germany), Aluminium nitrate nonahydrate, Sodium carbonate, and Sodium hydroxide (Sigma–Aldrich, Germany), Toluene, 2-aminopropylethoxysilane(APTES)(Sigma-Aldrich,Germany). Methanol,dimethylformamide (DMF) and terephthalic acid were used without further purification.

2.2 Synthesis of CoZnAl-LDH

The CoZnAl-LDH intercalated with carbonate was synthesised by the method used in[1, 19]. Typically, a mixed solution (400 mL) containing $Co(NO_3)_2.6H_2O$ (0.02mol/L), $Zn(NO_3)_2.6H_2O$ (0.02mol/L) and $Al(NO_3)_3.9H_2O$ (0.02mol/L) was added dropwise to a vigorously stirred mixed solution (400 mL) of NaOH (0.1mol/L) and Na_2CO_3 (0.02mol/L) at 40 ºC. The resulting gel was aged for 21 h under continuous stirring to allow for crystal growth. The crystals were then washed

repeatedly with deionised water by centrifuging at 4000 rpm for 5 min., followed by drying at 90 ºC for 17 h. The final product was called CoZnAl–CO_3 LDH and preserved for further use.

2.3 Synthesis of Co-MOF

Cobalt nitrate hexahydrate $(CoNO_3)_2.6H_2O$ (0.0138mol) and terephthalic acid (0.0138 mol) were dissolved in 80 mL of dimethylformamide (DMF) with mild stirring. The system was sealed and refluxed for eight hours at 100 ºC. Resulting crystals were collected by centrifugation, washed with methanol at least three times and oven dried at 75 ˚C for 45minutes and preserved for further use.

2.4 Modification of LDH

202.8 mg of carbonate intercalated CoZnAl -LDH was added to a 250 mL three-neck reaction flask containing 40 mL of toluene and 10 mL of (3-aminopropyl) triethoxysilane [APTES]. The mixture was heated to refluxing temperature for 4.5 h and was cooled for 30 minutes. The resulting liquid mixture was alternately centrifuged and washed with toluene methanol for three times. The residue was oven-dried at 70 ºC overnight.

2.5 Postsynthetic modification of Co-MOF

193.9 mg of APTES-modified CoZnAl -LDH was suspended in 40 mL of toluene and stirred. 169.8mg of Co-MOF was added to the mixture and was brought to a refluxing temperature. The mixture was refluxed for 4.5 h, cooled under stirring and the resulting product was alternately centrifuged for 3 minutes and washed with toluene and methanol for three times. The post-synthetic modified product was dried at 90 ºC overnight.

2.6 Characterization

The as-synthesised CoZnAl–CO_3 LDH, MOF, APTES-LDH and postsynthetic modified Co-MOF were characterized for the associated functional groups using Fourier transform infrared (FTIR) spectrometer (Spectrum Two, Perkin Elmer Instruments, USA) in the scanning range of 400–4000 cm^{-1}. Their crystalline nature was characterised using *X*-ray diffractometer (XRD-7000, Shimadzu, Japan). Thermo-gravimetric analysis (TGA) for thermal stability was carried out using a Perkin-Elmer TGA 4000 (Perkin Elmer Instruments, USA) using a heating rate of 10 °C min^{-1}.

2.7 Sorption Experiments

Analytical grade lead nitrate $(Pb(NO_3)_2)$ was used for stock solution (500 mg/L) preparation in this study. The uptake of Pb ions by postsynthetic modified (PSM) Co-MOF was observed with respect to a time interval of 1-120 min; pH in the range of 3–8; concentration of 20–140 mg/L, and temperature of 25–65 ºC. 20 mg of the adsorbent; and 20 mL of 40 mg/L Pb solution were shaken for 120 min at 200 rpm. pH of working solutions was adjusted by adding drops of either 0.1 M HCl or NaOH. At the end of each cycle supernatants were collected after centrifuging and residual concentration was determined using flame atomic absorption spectrophotometer (F-AAS, Shimadzu AA-7000, Japan).

2.8 Data Analysis

The experimental data of adsorption of Pb ions onto the postsynthetic modified Co-MOF was analysed using equilibrium and kinetic sorption models. The quantity of Pb ions adsorbed was determined using the material balance equation (1) as given by

$$q_e = \frac{V}{M}(C_o - C_e) \quad (1)$$

with q_e as the metal uptake capacity (mg/g of adsorbent at equilibrium), C_e the metal ion concentration in solution (mg/L) at equilibrium; C_o is the initial metal ion concentration (mg/L); V is the volume of solution in litres (L) and M, is the dry weight of adsorbent used (g).

The equilibrium of the adsorption processes was investigated and analysed using Langmuir, Freundlich and Temkin models.

The Freundlich isotherm applied to data is given in equation (2)

$$q_e = K_F C_e^{1/n} \quad (2)$$

where K_F is the Freundlich isotherm constant, n is the adsorption intensity factor and C_e is the solution phase concentration at equilibrium (mg/L).

The Temkin plot for sorption data was done using the equation (3)

$$q_e = \frac{RT}{b_T}\ln(K_T C_e) \quad (3)$$

where K_T is the Temkin isotherm constant (dm^3g^{-1}) and b_T is the adsorption potential of the adsorbent ($Jmol^{-1}$).

3. Results and Discussion

3.1 Characterization Studies

3.1.1 FTIR analysis

Functional group analysis of the precursors and post synthetic modified adsorbent was done with FT-IR and the spectra are shown in Figure 1.

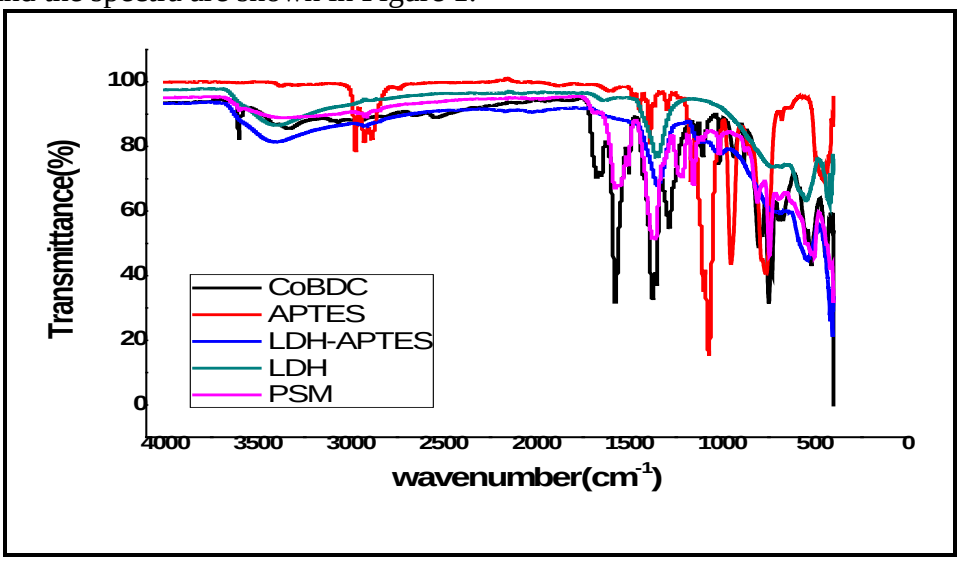

Figure 1. FT-IR spectra of precursors and product of postsynthetic modification of Co-MOF

The post-synthetic modified MOF showed bands that are shifted from the precursor band and peak values, indicating that there was an interactive product from the post synthetic modification protocol. The bands around 3406 cm^{-1}, 3396 cm^{-1}, 3325 cm^{-1} and 3356 cm^{-1} represents H-bonded stretching vibrations of O-H groups in LDH-APTES, LDH, CoBDC precursors and the PSM product respectively. However, the spectral intensity of the band for the PSM product is different and redshifted from those of the precursors. The signals at 1565 cm^{-1} and 1363 cm^{-1} of the CoBDC spectra, are assigned to the asymmetric and symmetric stretch of the C–O bond in the metal-bonded carboxyl group, which are characteristic of MOFs[20]. These peaks are redshifted in the PSM spectra to 1556 cm^{-1} and 1373 cm^{-1} respectively: this goes to indicate the successful interaction by the postsynthetic modification. The peak at 1223 cm^{-1} is assigned to the C-H in-plane bending vibrations of the benzene rings[20, 21] of the benzene dicarboxylic acid (BDC) of the precursor MOF moiety. The peak at 748 cm^{-1} is the out-of-plane bending vibrations of the C-H group of the benzene ring of the BDC. The fingerprint peak at 518 cm^{-1} represents the Co-O stretching vibration. The peaks around 1072 cm^{-1} corresponds to the SiO-H bond; that about 941 and 770 cm^{-1} are the Si-O-H and Si-O-Si bonds, respectively[22].These spectral values are within or close to other reports of composites of LDH/MOF[23]

3.1.2 PXRD analysis

The powder x-ray diffractograms of the LDH, LDH-APTES and the PSM Co-MOF are given in Figure 2.

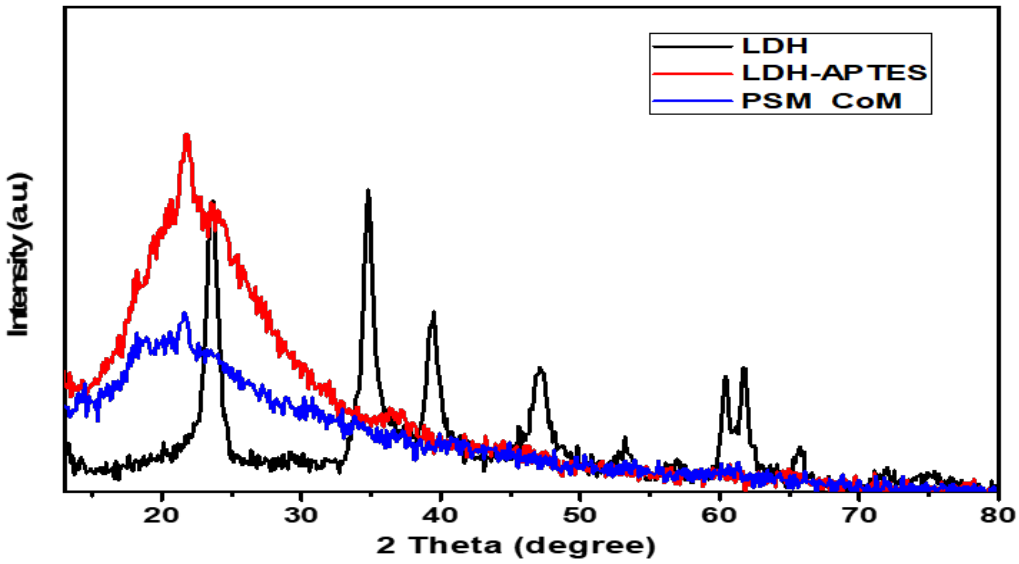

Figure 2. X-ray diffractograms of precursors and product of postsynthetic modification of Co-MOF

Sharp, characteristic diffraction peaks of the LDH which expresses its polycrystalline nature are found at 2θ angles of 23.66º, 34.8º, 39.47º, 47.37º, 60.35 and 61.9º, which corresponds to d-spacing of 3.8Å, 2.6Å, 2.3Å,1.9Å, 1.5Å and 1.5Å respectively. The broad and less intense peak of the post synthetic modified (PSM) Co-MOF at 2θ = 21.68º with a d-spacing of 4.1Å suggests that it is more amorphous than the precursors. The LDH-APTES showed a high intensity peak at about the same 2θ with the PSM. The lower intensity Co- MOF (PSM) at about the same 2θ angle with the secondary precursor, LDH-APTES, could imply the presence of an added component, which is the Co-BDC that was reacted with it. This then, like the case of the FTIR analysis points to the successful modification of the Co-BDC by the LDH-APTES.

3.1.3 TGA/DTA analyses

The mass loss and thermal stability of the postsynthetic modified Co-MOF were determined with the thermogravimetric and differential thermal (TGA/DTA) analyses, which are shown in Figure 3.

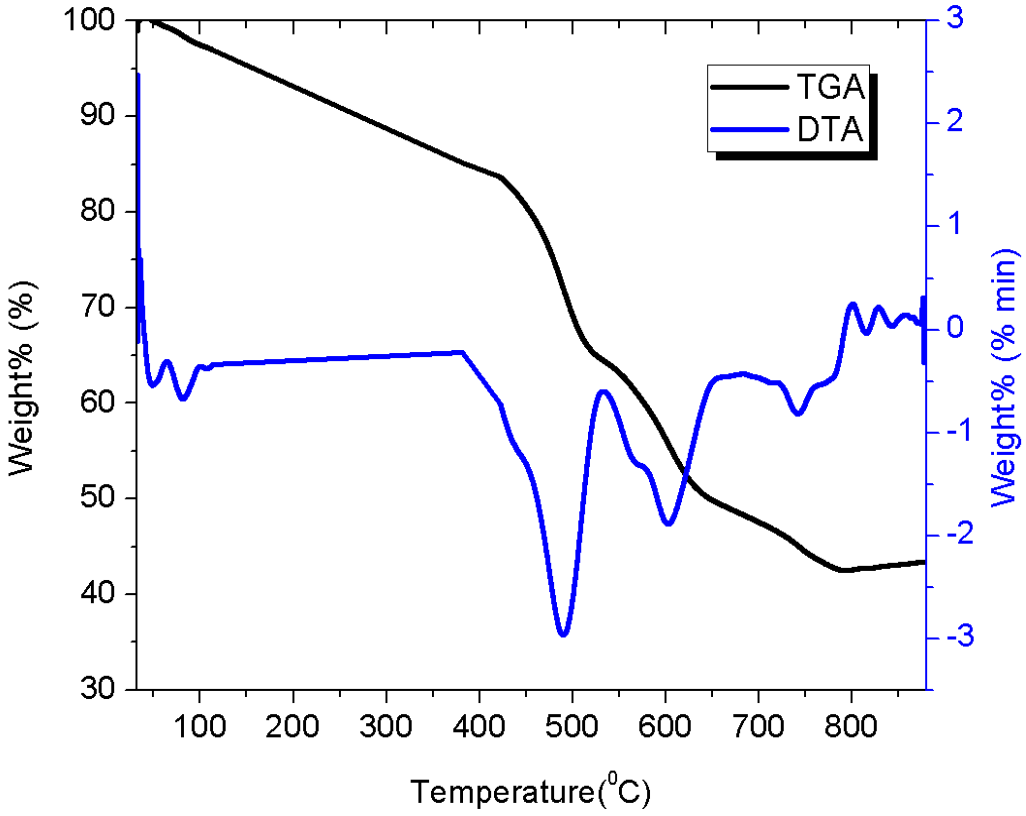

Figure 3. TGA/DTA of postsynthetic modified Co-MOF

The thermal profile of the postsynthetic modified product shows two minor and two major endothermic decomposition stages. The two minor points are at 81.9 ºC and 740.2 ºC. Decomposition points are found at 491.6 ºC and 613.8 ºC,though, they are less than the last two points.The initial minor transition at 81.9 ºC may be due to the loss of water; the major decomposition stage at 491.6 ºC can be ascribed to decomposition of surface OH^- and anions in the LDH matrix, while that at 613.8ºC corresponds to the decomposition of the organic linkers [24]. The decomposition stages at 491.6 ºC and 613.8 ºC. suggest that the PSM product has high thermal stability.

3.2 Effects of Physicochemical conditions applied to adsorption

3.2.1 Effect of Time on Adsorption

The effect of time on the adsorption of Pb by postsynthetic modified Co-MOF is shown in Figure 4.

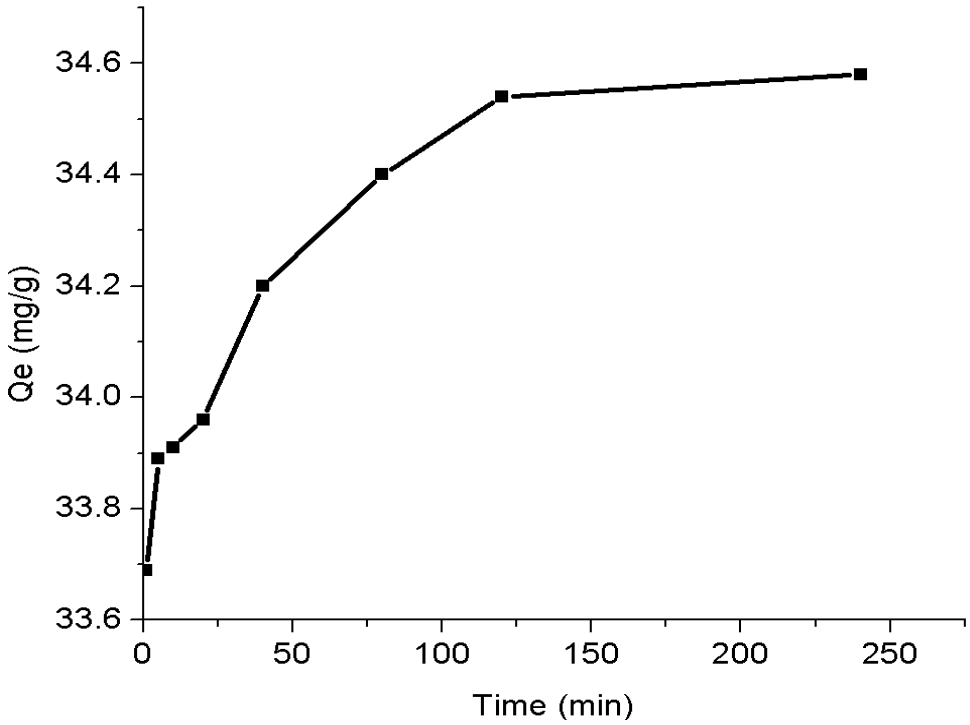

Figure 4. Effect of time on the adsorption of Pb ions by postsynthetic modified Co-MOF

The removal rate follows a nearly parabolic rise with time to the point when the curve begins to flatten to indicate the time of equilibrium. Equilibrium time was attained from 120 min. The plateau of the time plot indicates the coverage of available sites and internal pores in the material. The slow rate of attainment of equilibrium may be ascribed to the presence of a large number of sites on the adsorbent for adsorption[21]. Adsorption capacity with respect to time at equilibrium was 34.58 mg/g, representing 87% of adsorbate uptake by the PSM Co-MOF.

3.2.2 Effect of initial metal ion concentration on Adsorption

The effect of initial metal ion concentration is represented on the plot in Figure 5.

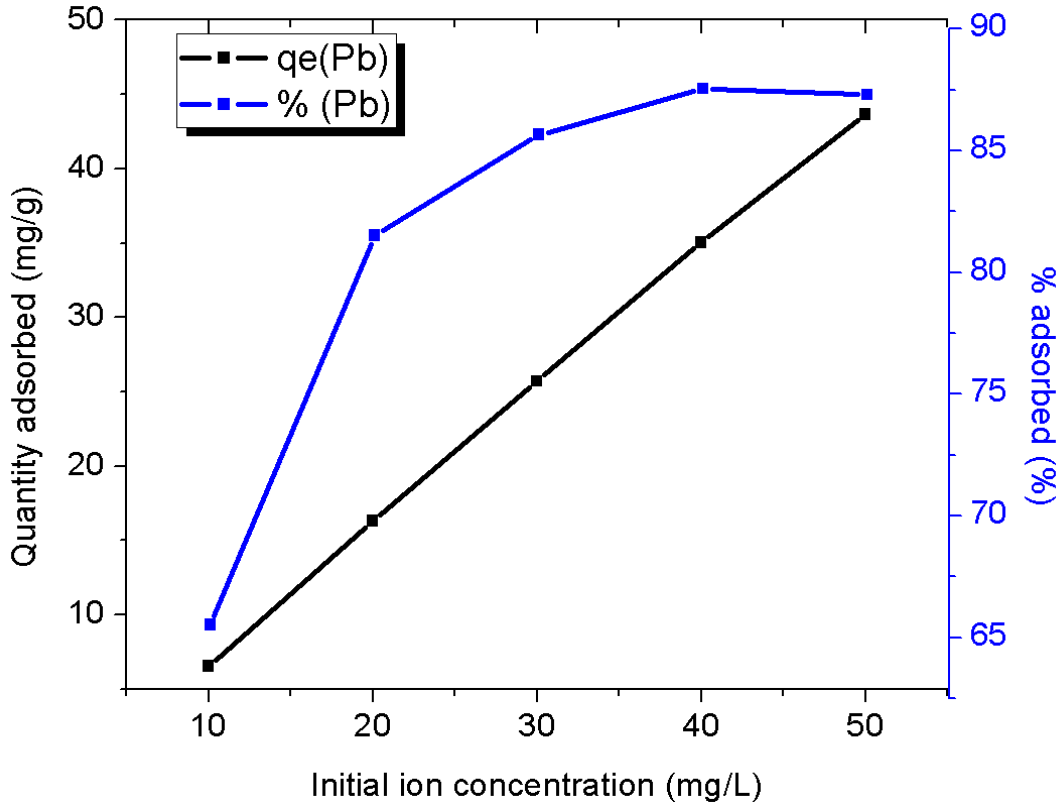

Figure 5. Effect of initial ion concentration on the adsorption of Pb ions by postsynthetic modified Co-MOF

The result indicates a linear increase of adsorption with initial metal ion concentration for the range of concentration chosen. This behaviour can be attributed to the availability of vacant sites on the PSM adsorbent for the uptake of the Pb ions in solution. The secondary plot of % adsorption indicates a saturation of sites at higher concentration.

3.2.3 Effect of pH on Adsorption

The results (in Figure 6) of the pH study on the postsynthetic modified MOF showed that adsorption increased with increase in pH up to a maximum before a descent. Maximum adsorption pH was 6 with a capacity of 34.99 mg/g. Favourable uptake of Pb by the PSM product can therefore occur at pH $\leq$ 6.

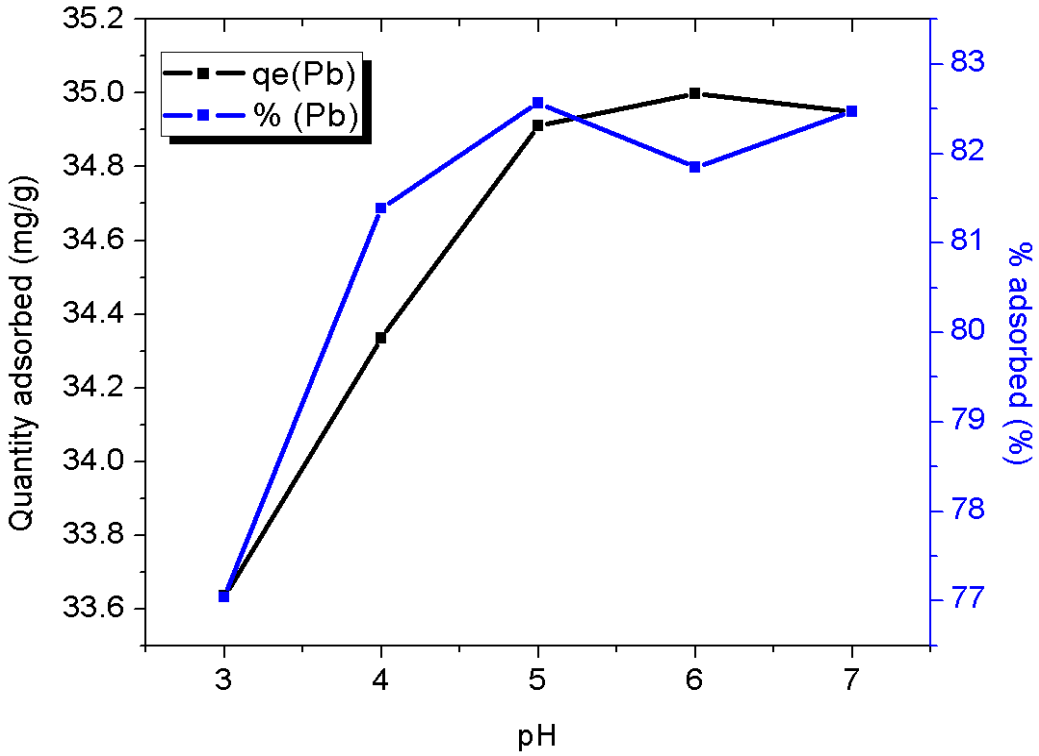

Figure 6. Effect of pH on the adsorption and % removal of Pb ions by postsynthetic modified Co-MOF

3.3 Adsorption Isotherms

Two adsorption isotherms were used for the equilibrium modelling of the adsorption of Pb ions by PSM. The data from the adsorption experiments were fitted into, Freundlich and Temkin model equations to assess the adsorption capacity and heat of sorption of the PSM product. The results of the modelling are shown in Figure 7 and the isotherm parameters are given in Table 1. The results show that the Temkin isotherm followed closest to the experimental isotherm than the other models (R^2 = 0.9544). This implies then that, adsorbent-adsorbate interaction was significant at the range of concentration used for the adsorption, hence, the PSM adsorbed the Pb ions significantly.

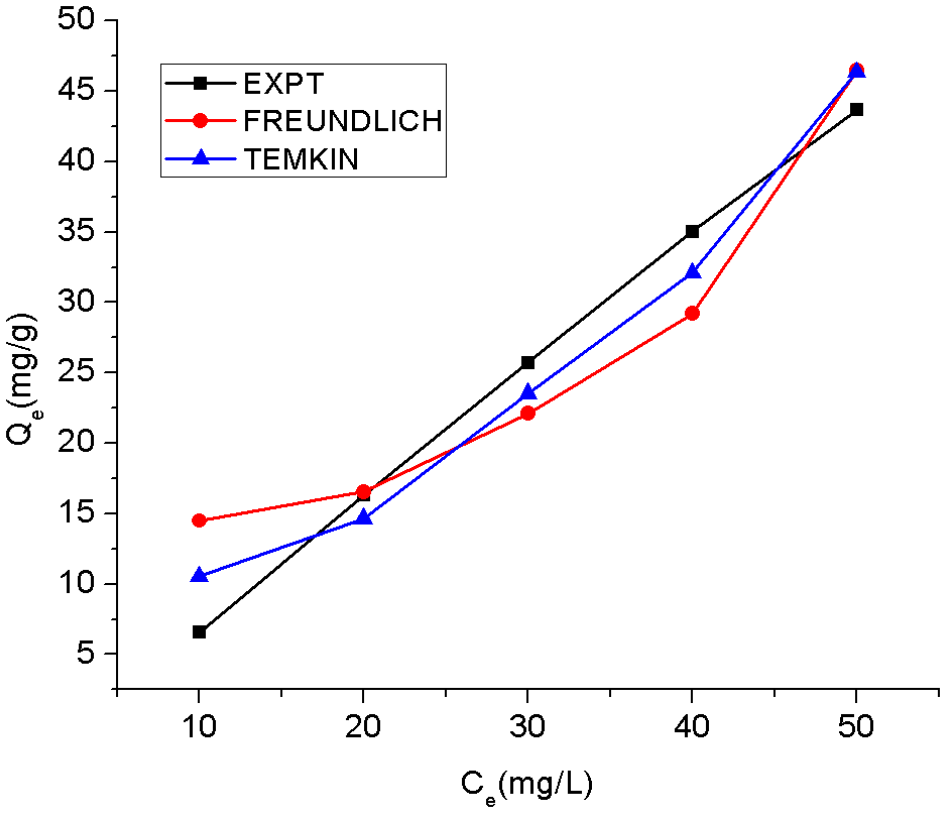

Figure 7. Equilibrium isotherms for the adsorption of Pb ions by postsynthetic modified Co-MOF

Table 1. Isotherm Parameters of Adsorption of Pb ions by Postsynthetic modified Co-MOF

Isotherm	Parameters	Values
Freundlich	$K_F(mg/g)(L/g)^{-1/n}$ n R^2	1.3661 0.5243 0.8635
Temkin	$K_T(dm^3/g)$ $b_T(J/mol)$ R^2	58.6420 0.3472 0.9544

3.4 Adsorption Kinetics

Two kinetic models namely, Lagergren pseudo-first order(PFO) and the pseudo-second order (PSO)[25] rate equations, were fitted to adsorption data to verify the prevailing mechanism. These are given in equations 4 and 5.

The pseudo-first order rate equation is given as:

$$\ln(q_e - q_t) = -k_1 t + lnq_e \quad (4)$$

The pseudo-second order(PSO) kinetic model is represented as

$$\frac{t}{q_t} = \frac{t}{q_e} + \frac{1}{k_2 q_e^2} \quad (5)$$

The models are plotted with respect to time in Figure 8 and the kinetic parameters for the models are given in Table 2.

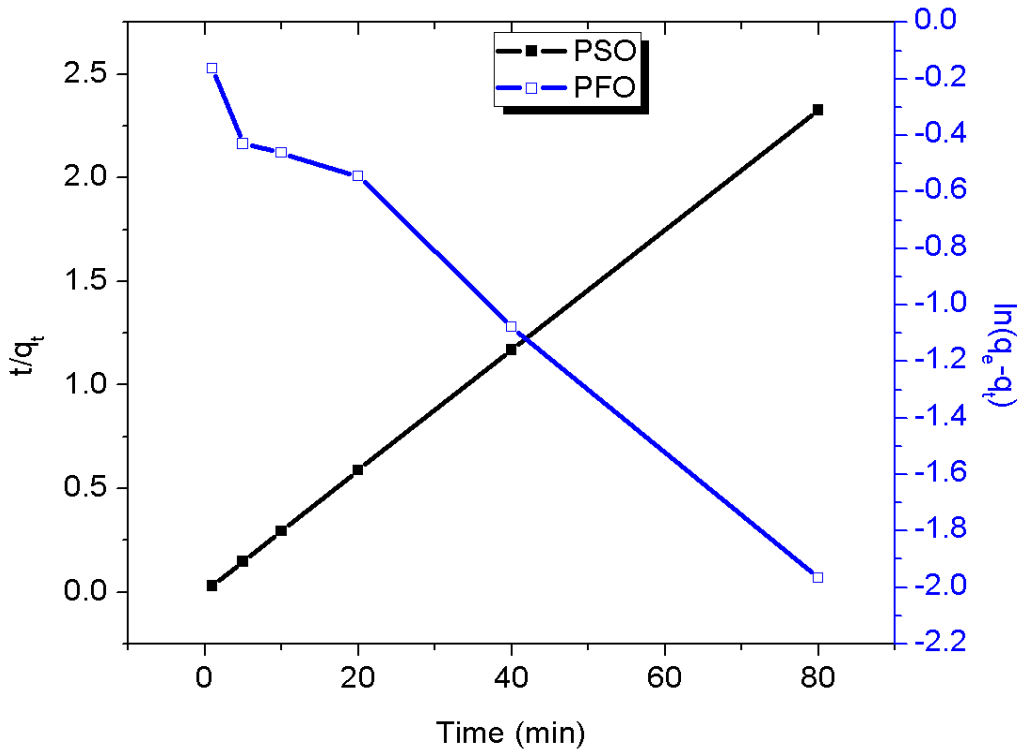

Figure 8. Pseudo first order and pseudo second order kinetics plot for the adsorption of Pb ions by postsynthetic modified Co-MOF

Table 2. kinetic Parameters of Adsorption of Pb ions by Postsynthetic modified Co-MOF

Model	Parameter	Value
	$q_e(expt)$[mg/g]	34.40
PFO	k_1 $q_e(calc)$[mg/g] R^2	0.0218 0.813 0.9866
PSO	k_2 q_e(calc)[mg/g] R^2	0.2117 34.36 1.000

From the values of the parameters in the table, it was observed that the correlation coefficient, R^2, of the PSO is higher than that of the PFO thus making PSO a better fitting model. It was also observed that, there was no significant difference between the qe (exp) and the q_e (calc) of the PSO, thus making it the prevailing rate mechanism of the sorption process[26].

The PFO equation represents an exponential decay process in which the reactant is likely consumed; and since PFO and PSO are functions of time, the PSO equation could represent a simultaneous or complementary growth, in which a product is formed on the adsorbent surface. The PFO rate mechanism could be considered as the release of adsorbate materials from the bulk for onward growth of the product on the adsorbent by surface attachment. The two rate mechanisms are all functions of time and are competitive in any adsorption process. The results from Table 2 shows that the rate

constant for the PFO is negative (k_1 = -0.0218) implying a decreasing or depleting amount of Pb ions from the bulk solution. The rate constant for the PSO on the other hand is greater than zero (k_2 = 0.2103), which implies an increasing amount of Pb ions or growth on the adsorbent (PSM) surface. Thus, the Pb ions were increasingly depleted from bulk and moved to the adsorbent surface for adsorption.

3.5 Diffusion Analysis

Movement of adsorbate particles to adsorbent surface is made possible by bulk and surface processes such as: (i) the bulk solution diffusion of adsorbate from solution to the boundary layer of solution surrounding the adsorbent particles; film diffusion of adsorbate particles through the liquid film surrounding the adsorbent particles; and (iii) diffusion of adsorbate particles into the adsorbent pores and adsorption on available sites. One or more of these processes can be involved in the adsorption process; the slowest process controls the rate of adsorption[27].

Two diffusion models were used for the analysis of the adsorption data: Weber-Morris intraparticle diffusion[28] and film diffusion which are given as the equations 6 and 7 respectively

$$q_t = k_{id} t^{1/2} + I \quad (6)$$

Where k_{id} is the intra-particle diffusion rate constant (mg g^{-1} min^{-1}) and I (mg g^{-1}) is a constant that describes the thickness of the boundary layer

$$\ln(1-\propto) = -k_{fd} t \quad (7)$$

where $\propto$ is the fractional attainment of equilibrium ($\propto = {}^{q_t}/_{q_e}$), k_{fd} is liquid film diffusion constant. The results are shown in Figure 9 and 10.

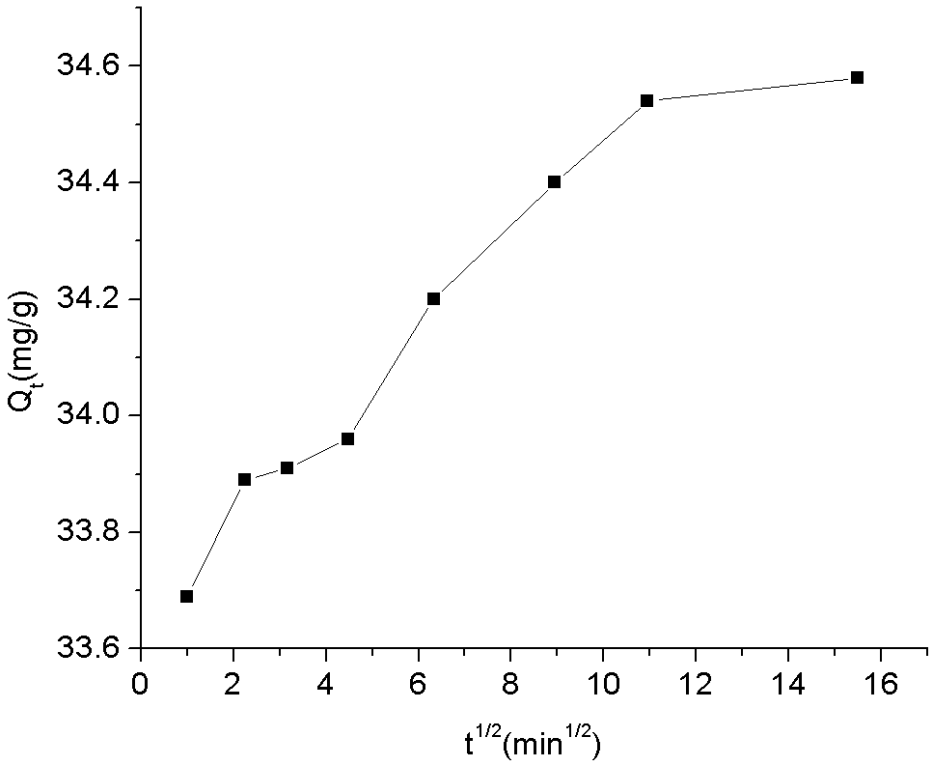

Figure 9. Weber-Morris intra-particle diffusion plot for the adsorption of Pb ions by postsynthetic modified Co-MOF

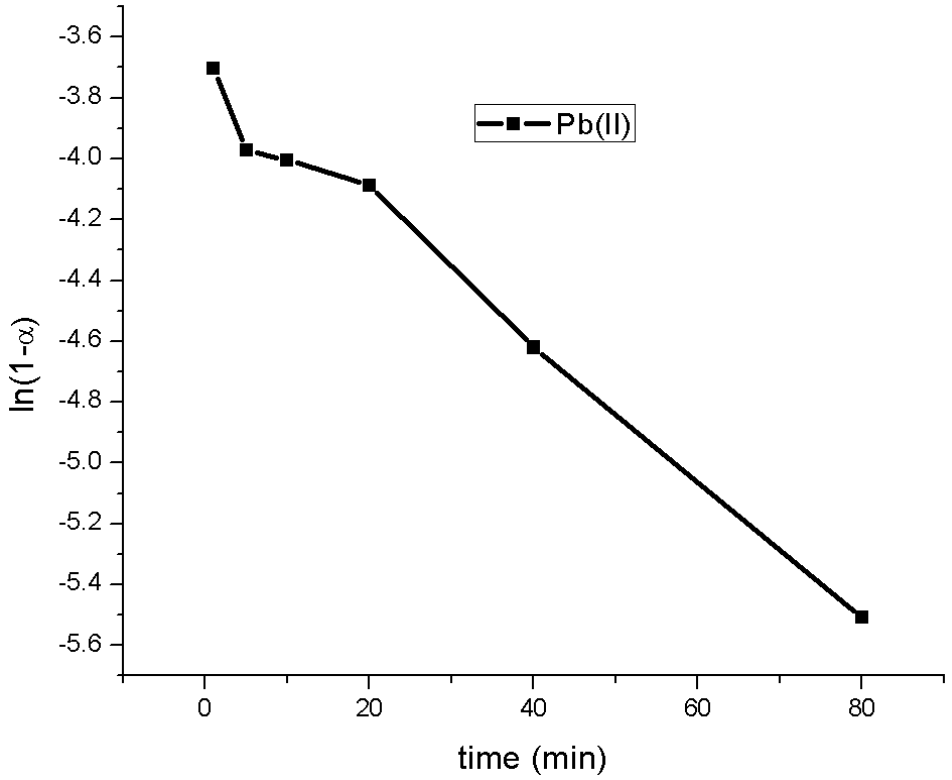

Figure 10. Film diffusion plot for the adsorption of Pb ions by postsynthetic modified Co-MOF

The plot for Weber-Morris intraparticle diffusion is multilinear and therefore implies that, it is not the rate controlling diffusion process[29, 30]. However, the intraparticle diffusion step has an R^2 value of 0.9917, which means that it was significant, but not a controlling step of the adsorption. The diffusion model parameters of adsorption are given in Table 3.

Table 3. Diffusion Parameters of Adsorption of Pb ions by Postsynthetic modified Co-MOF

Diffusion Model	Parameter	Value
Weber-Morris IPD	$k_{id}\ (mgg^{-1}min^{-1})$	0.0648
	$I(mg/g)$	33.72
	R^2	0.9224
Film diffusion	k_{fd}	-0.0218
	R^2	0.9866

4. Conclusion

An ex-situ postsynthetic modification of Co-MOF with an amino-silane modified layered double hydroxide (LDH) was carried out and applied in the removal of Pb ions from aqueous solution. Characterisation studies showed that the postsynthetic modification was successful**.** Blueshifts and redshifts of existing FT-IR bands in the PSM product in relation to that of the precursors confirmed the modification. Thermal stability test indicated that the PSM product was stable at temperatures up to 400 ºC after a slight loss of surface water at low temperatures. Crystallinity of the PSM product was however lower than that of the precursors as indicated by the diffractograms. Equilibrium data was better correlated by the Temkin model with a heat of sorption at 33.72 J/mol. Rate data was better

correlated with the pseudo second-order kinetic model. Adsorption capacity of PSM product from kinetic studies put qe at 34.5mg/g of adsorbent. The multilinearity of the Weber-Morris intraparticle diffusion plot indicated that the diffusion consisted of more than two steps, and so the intraparticle diffusion was not the rate limiting step. The film diffusion plot gave an R^2 value of 0.9866 which is greater than that of the intraparticle diffusion (0.9224), which then implies that, it has a more significant control of the diffusion process.

Acknowledgements

The authors are grateful to the Research Directorate of the Vaal University of Technology, Vanderbijlpark, South Africa for the research funding support.

References

[1] Abasi, C.Y., Ejidike, I.P. and Dikio, E.D., (2018) Synthesis, characterisation of ternary layered double hydroxides (LDH) for sorption kinetics and thermodynamics of Cd^{2+}, International Journal of Environmental Studies, 1-15.
[2] Shan, R.R., Yan, L.G., Yang, K., Hao, Y.F. and Du, B., (2015) Adsorption of Cd(II) by Mg-Al-CO3- and magnetic Fe_3O_4/Mg-Al-CO_3-layered double hydroxides: Kinetic, isothermal, thermodynamic and mechanistic studies, J Hazard Mater, 299, 42-49.
[3] Tchounwou, P.B., Yedjou, C.G., Patlolla, A.K. and Sutton, D.J. (2012) Heavy metal toxicity and the environment, Exp Suppl, 101, 133-164.
[4] Masindi, V. and Muedi, K.L., (2018) Environmental Contamination by Heavy Metals, in: H.E.-D.M. Saleh (Ed.) Heavy Metals, IntechOpen, http://www.intechopen.com/download/pdf/pdfs_id/60680
[5] Abasi, C.Y., Orodu, V.E. and Abia, A.A. (2017) Effect of pH on sorption of Pb on Raphia Palm Fruit., International Journal of Current Research in Life Sciences, 06, 679-684
[6] Cao, Y., Khan, A., Kurniawan, T.A., Soltani, R. and Albadarin, A.B. (2021) Synthesis of hierarchical micro-mesoporous LDH/MOF nanocomposite with in situ growth of UiO-66-(NH2)2 MOF on the functionalized NiCo-LDH ultrathin sheets and its application for thallium (I) removal, Journal of Molecular Liquids, 336, 116189.
[7] Tanabe, K.K. and Cohen, S.M. (2011)Postsynthetic modification of metal-organic frameworks--a progress report, Chem Soc Rev, 40 , 498-519.
[8] Liu, Y., Wang, N., Diestel, L., Steinbach, F. and Caro, J. (2014) MOF membrane synthesis in the confined space of a vertically aligned LDH network, Chem Commun (Camb), 50 4225-4227.
[9] Ahmed, I. and Jhung, S.H. (2014) Composites of metal–organic frameworks: Preparation and application in adsorption, Materials Today, 17 136-146.
[10]. Theiss, F.L, Ayoko G.A.and Frost, R.L. (2016) Synthesis of layered double hydroxides containing Mg^{2+}, Zn^{2+}, Ca^{2+} and Al^{3+} layer cations by co-precipitation methods—A review, Applied Surface Science, 383, 200-213.
[11] Wu, S.-C., Chang, P.-H., Chou, S.-H., Huang, C.-Y., Liu, T.-C. and Peng, C.-H. (2020) Waffle-Like Carbons Combined with Enriched Mesopores and Highly Heteroatom-Doped Derived from Sandwiched MOF/LDH/MOF for High-Rate Supercapacitor, Nanomaterials 10, 1 - 15.
[12] Starukh, G. (2017) Photocatalytically Enhanced Cationic Dye Removal with Zn-Al Layered Double Hydroxides, Nanoscale Research Letters, 12, 391.
[13] Mohd Sidek, H.B., Jo, Y.K., Kim, T.W. Hwang, Y.K., Chang, J.-S. and Hwang, S.-J. (2017) Enhancement of the Water Adsorptivity of Metal–Organic Frameworks upon Hybridization with Layered Double Hydroxide Nanosheets, The Journal of Physical Chemistry C, 121, 15008-15016.

[14] Cao, F., Gan, M. , Ma, L., Li, X., Yan, F. , Ye, M., Zhai, Y. and Zhou, Y. (2017) Hierarchical sheet-like Ni–Co layered double hydroxide derived from a MOF template for high-performance supercapacitors, Synthetic Metals, 234, 154-160.
[15] Liu, Y., Wang, N., Pan, J.H., Steinbach, F. and Caro, J. (2014) In Situ Synthesis of MOF Membranes on ZnAl-CO3 LDH Buffer Layer-Modified Substrates, Journal of the American Chemical Society, 136, 14353-14356.
[16] Kalaj, M. and Cohen, S.M. (2020) Postsynthetic Modification: An Enabling Technology for the Advancement of Metal−Organic Frameworks, ACS Cent. Sci., 6, 1046−1057.
[17] Song, Y.F. and Cronin, L. (2008) Postsynthetic covalent modification of metal-organic framework (MOF) materials, Angew Chem Int Ed Engl, 47, 4635-4637.
[18] Liu, J.H., Pan, Y., Wang, N., Steinbach, F., Liu, X. and Caro, J. (2015) Remarkably enhanced gas separation by partial self-conversion of a laminated membrane to metal-organic frameworks, Angew Chem Int Ed Engl, 54, 3028-3032.
[19] Abasi, C.Y., Diagboya, P.N.E. and Dikio, E.D. (2018) Layered double hydroxie of cobalt-zinc-aluminium intercalated with carbonate ion:Preparation and Pb(II) ion removal capacity, International Journal of Environmental Studies, https://doi.org/10.1080/00207233.2018.1517935
[20] Rivera, J.M., Rincon, S., Ben Youssef, C. and Zepeda, A. (2016) Highly Efficient Adsorption of Aqueous Pb(II) with Mesoporous Metal-Organic Framework-5: An Equilibrium and Kinetic Study, Journal of Nanomaterials, 9.
[21] ElHassani, K.., Beakoua, B.H, Kalnina, D., Oukani, E.and Anouar, A. (2017) Morphological properties of layered double hydroxides on adsorption Applied Clay Science 140, 124–131.
[22] Saif, B., Wang,V., Chuan, D. and Shuang, S. (2015) Synthesis and Characterization of Fe_3O_4 Coated on APTES as Carriers for Morin-Anticancer Drug, Journal of Biomaterials and Nanobiotechnology, 06, 267-275.
[23] Soltani, R., Pelalak, R., Pishnamazi, M., Marjani, A. and Shirazian, S. (2021) A water-stable functionalized NiCo-LDH/MOF nanocomposite: green synthesis, characterization, and its environmental application for heavy metals adsorption, Arabian Journal of Chemistry, 14, 1 -11.
[24] Yang, Y., Yan, X., Hu, X., Feng, R.and Zhou, M. (2017) In-situ growth of ZIF-8 on layered double hydroxide- Effect of Zn-Al molar ratios on their structural, morphological and adsorption properties., Journal of Colloid and Interface Science 505, 206–212.
[25] Ho, Y.S. and McKay, G. (1999) Pseudo-second order model for sorption processes, Process Biochemistry, 34, 451-465.
[26] Akbar, N.A., Mohd Kamil, N.A.F., Md Zin, N.S., Adlan, M.N. and Aziz, H.A. (2018) Assessment of kinetic models on Fe adsorption in groundwater using high-quality limestone, IOP Conference Series: Earth and Environmental Science, 140, 012030.
[27] Singh, S.K., Townsend, T.G., Mazyck, D. and Boyer, T.H. (2012) Equilibrium and intra-particle diffusion of stabilized landfill leachate onto micro- and meso-porous activated carbon, Water Research, 46, 491-499.
[28] Weber, W.J. and Morris, J.C. (1963) Kinetics of adsorption carbon from solutions, Journal Sanitary Engeering Division Proceedings.American Society of Civil Engineers, 89, 31-60, .
[29] Olu-Owolabi, B.I., Diagboya, P.N. and Adebowale, K.O. (2014) Evaluation of pyrene sorption-desorption on tropical soils, Journal of Environmental Management 137 1-9.
[30] Qiu, H., Lu, L., Pan, B.-c., Zhang, Q.-j., Zhang, W.-m. and Zhang, Q.-x. (2009) Critical review in adsorption kinetic models, Journal of Zhejiang University-SCIENCE A, 10, 716-724.